JP5J.5 DAMAGING SURFACE WIND MECHANISMS WITHIN THE 10 JUNE 2003 SAINT LOUIS BOW ECHO DURING BAMEX

Nolan T. Atkins and Christopher Bouchard
Lyndon State College, Lyndonville, Vermont

Ron W. Przybylinski
National Weather Service, Saint Charles, Missouri

Robert J. Trapp
Purdue University, West Lafayette, Indiana

Gary K. Schmocker
National Weather Service, Saint Charles, Missouri

1. INTRODUCTION

It is well known that bow echoes often produce swaths of "straight-line" wind damage generally F0-F2 in damage intensity. Fujita (1978) first described the morphology of a radar-observed bow echo and its attendant damage. He described how downburst winds associated with rear inflow descend from an initial tall echo and push the convective cells outward at the apex of the developing bow. Downburst winds generated surface wind damage at the bow apex upon reaching the ground.

Recent observations and numerical simulations (e.g., Schmocker et al. 2000; Trapp and Weisman 2003) have suggested another mechanism that may produce damaging "straight-line" winds in bow echoes. Low-level meso-γ-scale vortices, or "mesovortices", formed on the leading edge of the bow echo may also produce swaths of straight-line wind damage *north* of the bow apex. Resolution of the damaging wind mechanism(s) within bow echoes requires the superposition of detailed data from damage surveys and Doppler radar. Such analyses have not been published in the literature.

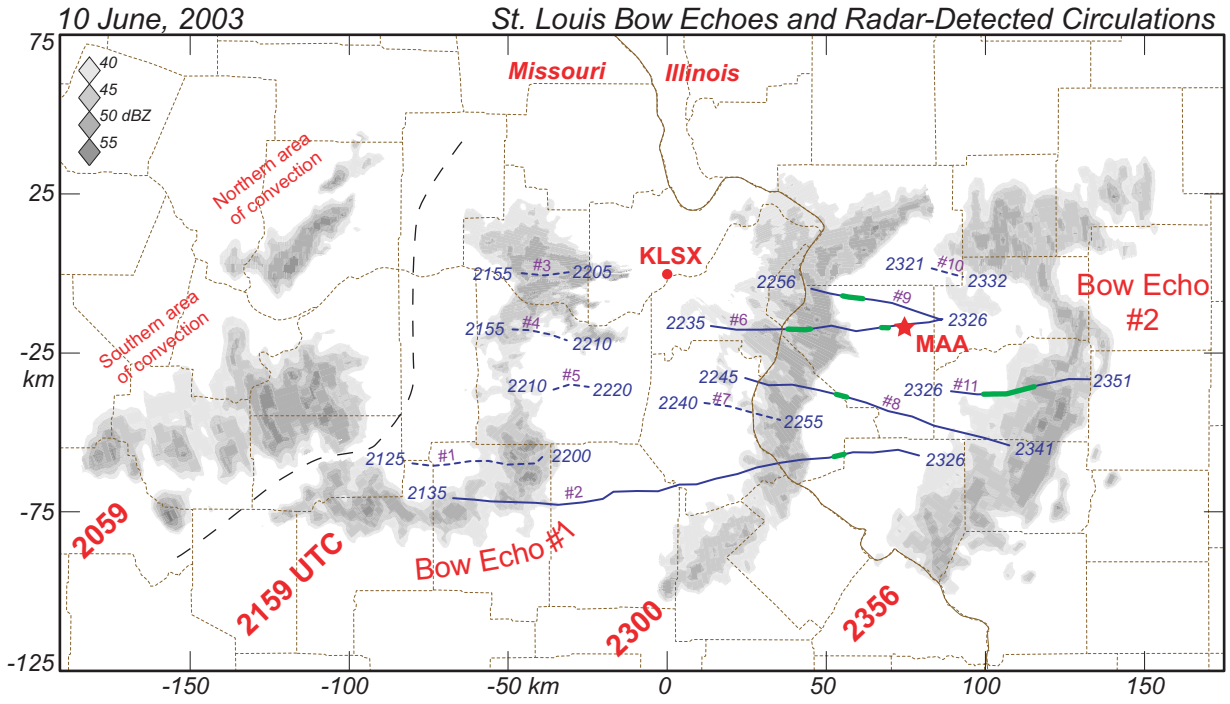

Figure 1. Radar reflectivity data at 0.5 degrees from the KLSX radar. Solid and short-dashed blue lines indicate positions of tornadic and nontornadic mesovortices, respectively. Tornado times are shown with thick green lines. The long dashed line separates the 2059 and 2159 UTC radar data.

**Corresponding Author Address*: Dr. Nolan T. Atkins, Department of Meteorology, Lyndon State College, Lyndonville, VT 05851; email: nolan.atkins@lyndonstate.edu

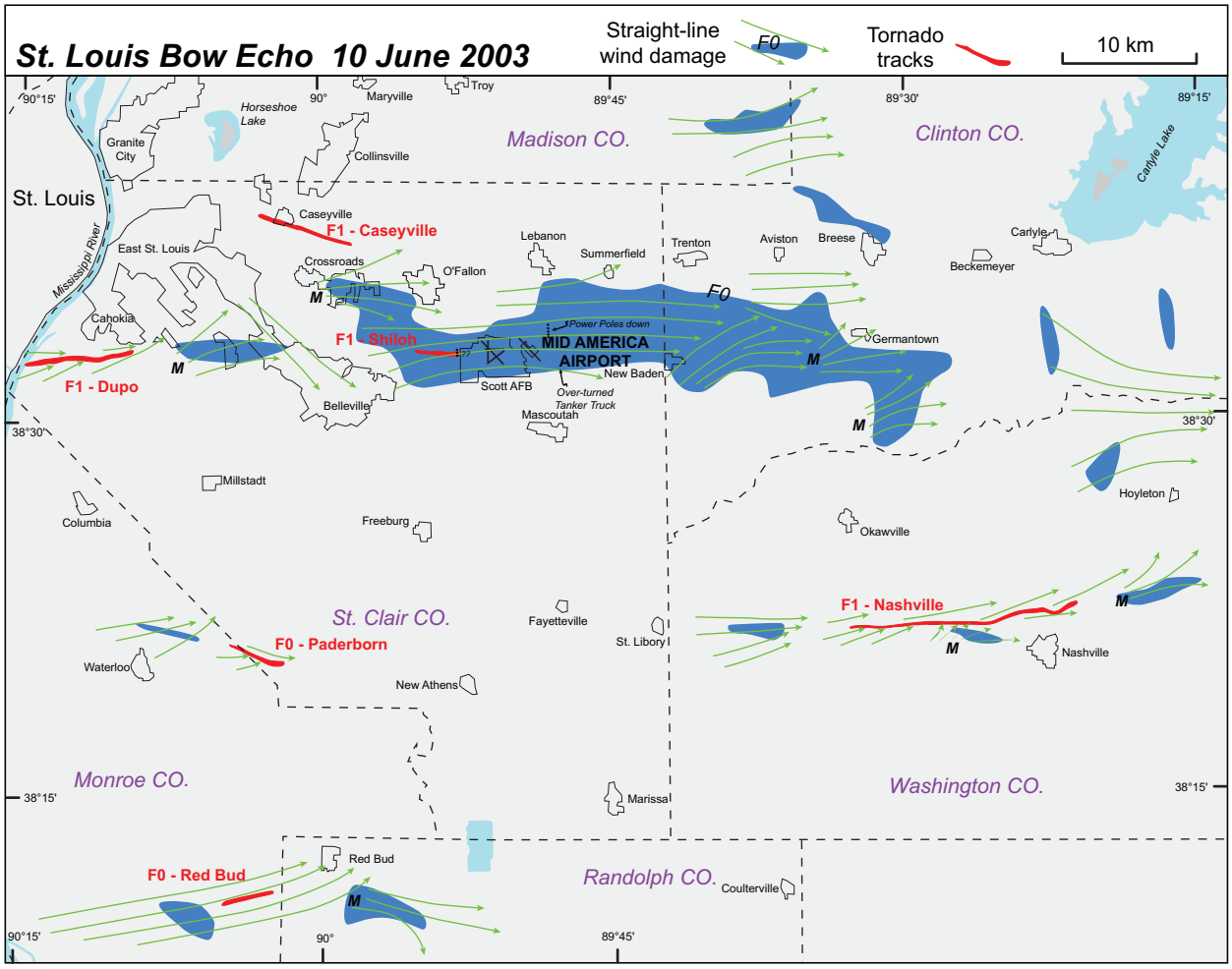

Figure 2. Damage survey analysis over southwestern Illinois. F-scale analysis is shown in blue. Streamlines of damaging winds based on direction of tree fall and building debris are shown in green. Tornado tracks are shown in red. Water (light blue), county lines (long dashed) and towns (solid thin) are also shown. Microburst locations are denoted by the "M"s.

The mesovortices have also been shown to produce tornadoes primarily at or north of the bow echo apex. Przybylinski et al. (2000) have shown that tornadic mesovortices often form at the intersection point of the primary convective system and a nearly perpendicular preexisting boundary. Previous studies (e.g., Funk et al. 1999; Przybylinski et al. 2000; Atkins and Przybylinski 2002; Atkins et al. 2004) have also shown that tornadic mesovortices are relatively strong at low levels and strengthen and deepen with time prior to tornadogenesis. Not all mesovortices, however, become tornadic. The structural differences between tornadic and nontornadic mesovortices are not well understood.

During the afternoon hours on 10 June, 2003, a damaging bow echo moved eastward over the greater Saint Louis area during the Bow Echo and MCV Experiment (BAMEX, Davis et al. 2004). BAMEX occurred from mid May through early July, 2003 and operated out of the Mid America Airport in Mascoutah, Illinois (location of star in Fig. 1). One of the objectives of BAMEX was to better understand how mesoscale convective systems (MCS) generate damaging winds. The MCS on 10 June 2003 produced a straight-line wind damage swath approximately 50 km in length and eleven mesovortices of which five were tornadic. The objectives of this study are to determine the mechanism that created the 50 km long damage swath and to examine the structural characteristics of the tornadic and nontornadic mesovortices.

2. RADAR EVOLUTION AND DAMAGE SURVEY

The MCS initiated over central Missouri at about 18 UTC, moved eastward and was located approximately 125 km west of the Saint Charles (KLSX) radar by 21 UTC (Fig. 1). The system subsequently produced two bow echoes, the first observed roughly 100 km southwest

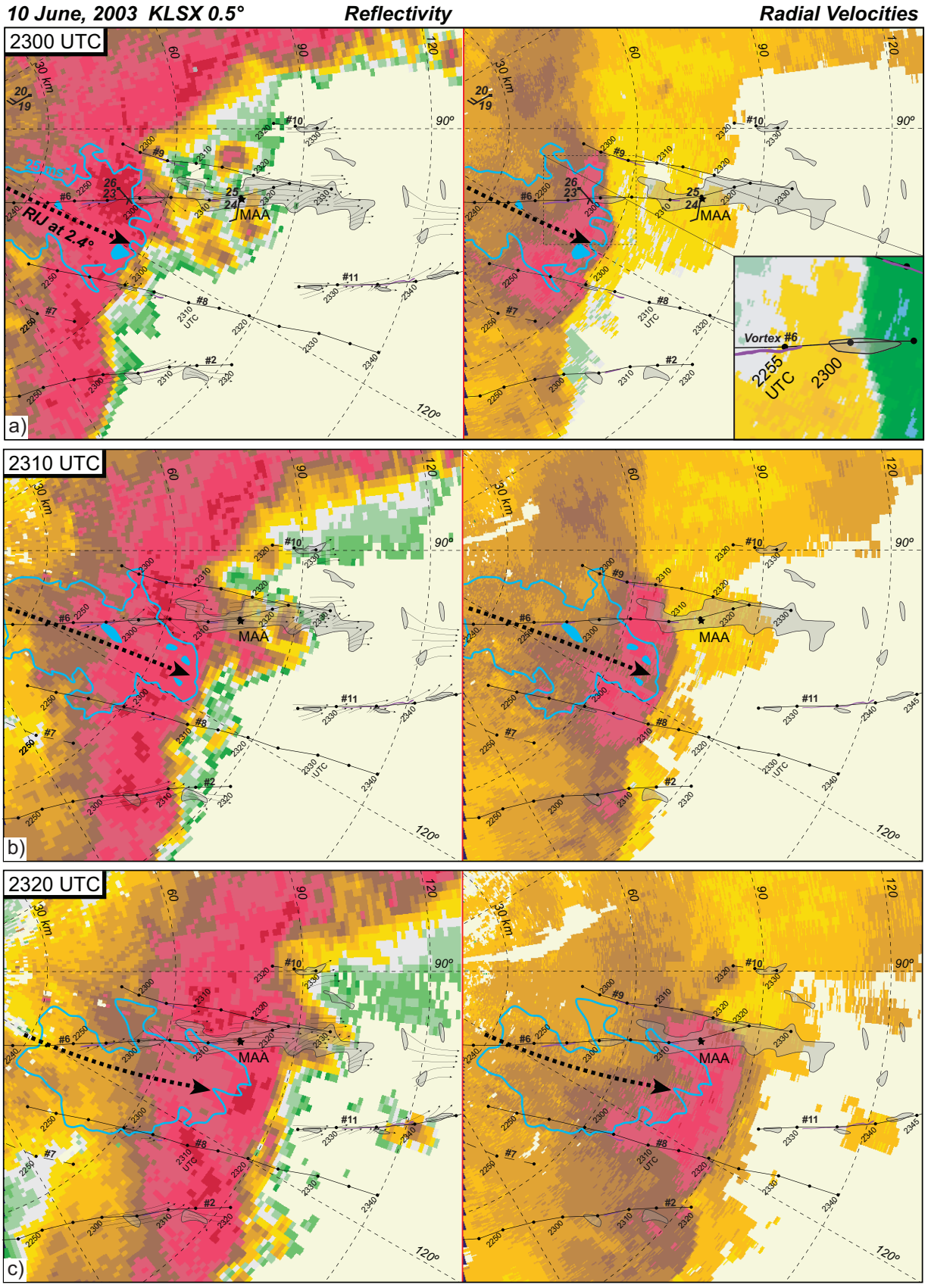
10 June, 2003 KLSX 0.5°
Reflectivity
Radial Velocities
2300 UTC
2310 UTC
2320 UTC
a)
b)
c)
RIJ at 2.4°
MAA
Vortex #6
2255 UTC
2300
30 km
20
19
90°
120°
60
90
120
#2
#6
#7
#8
#9
#10
#11
2310 UTC
2330 UTC

Figure 3. Damage survey data from Fig. 2 superimposed on radar reflectivity (dBZ) and Doppler velocities (ms^{-1}) at (a) 2300, (b) 2310, and (c) 2320 UTC. In all panels, F0 or greater straight-line wind damage is shown in gray, tornado tracks in purple, and streamlines in black. Mesovortex locations are shown as black lines. The 25 ms^{-1} radial velocity contour at 2.4 degrees is shown in blue. The approximate location of the RIJ is shown as a thick dashed black line. MAA is the location of the Mid America Airport.

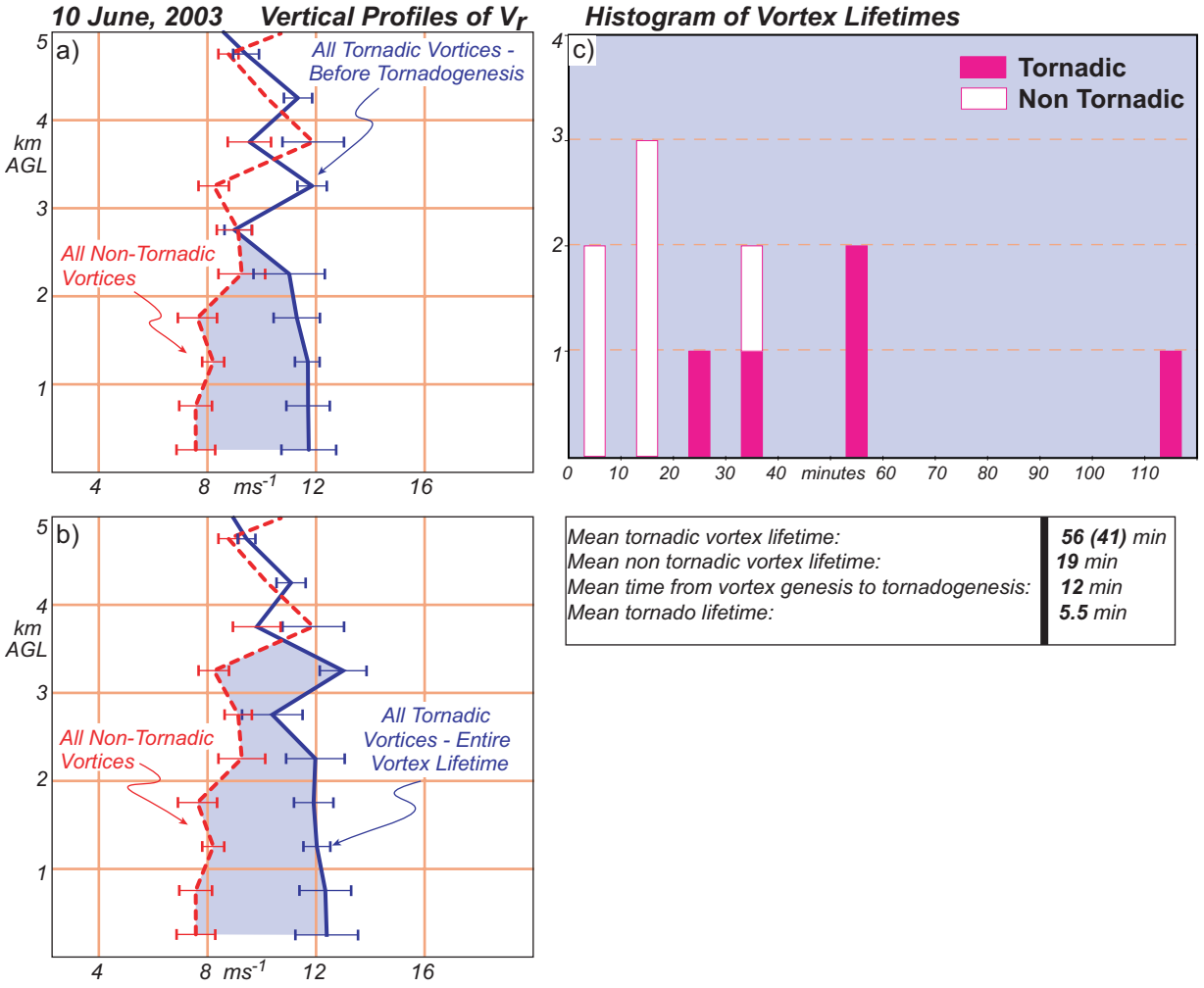

Figure 4. Mean profiles of Vr for the tornadic and nontornadic vortices shown in Fig. 1. Error bars are one standard deviation. Vr is defined as the average of the absolute values of the outbound and inbound couplet maximum. Only data prior to tornadogenesis was used in (a) while all data was used for the tornadic vortices in (b). (c) Histogram of lifefimes for all of the tornadic and non tornadic vortices shown in Fig. 1.

of the radar (well defined at 2159 UTC) and the second later on in southwestern Illinois. The MCS also produced many tornadic (solid lines) and nontornadic (short dashed lines) mesovortices.

A detailed aerial and ground damage survey of this event was performed. Damage produced by the second bow echo in Fig. 1 is shown in Fig. 2. Clearly evident is a primary damage swath of F0 or greater intensity that was about 50 km in length and 8 km in width. The damage began approximately at 2300 UTC and ended one hour later. Note that the BAMEX Operations Center at Mid America Airport (MAA) was directly in the damage path! Damage survey efforts also uncovered six F0-F1 tornadoes in southwestern Illinois associated with this convective system.

3. DAMAGING WIND MECHANISMS

In order to understand the mechanism(s) creating the 50 km long damage swath in Fig. 2, the damage sur-

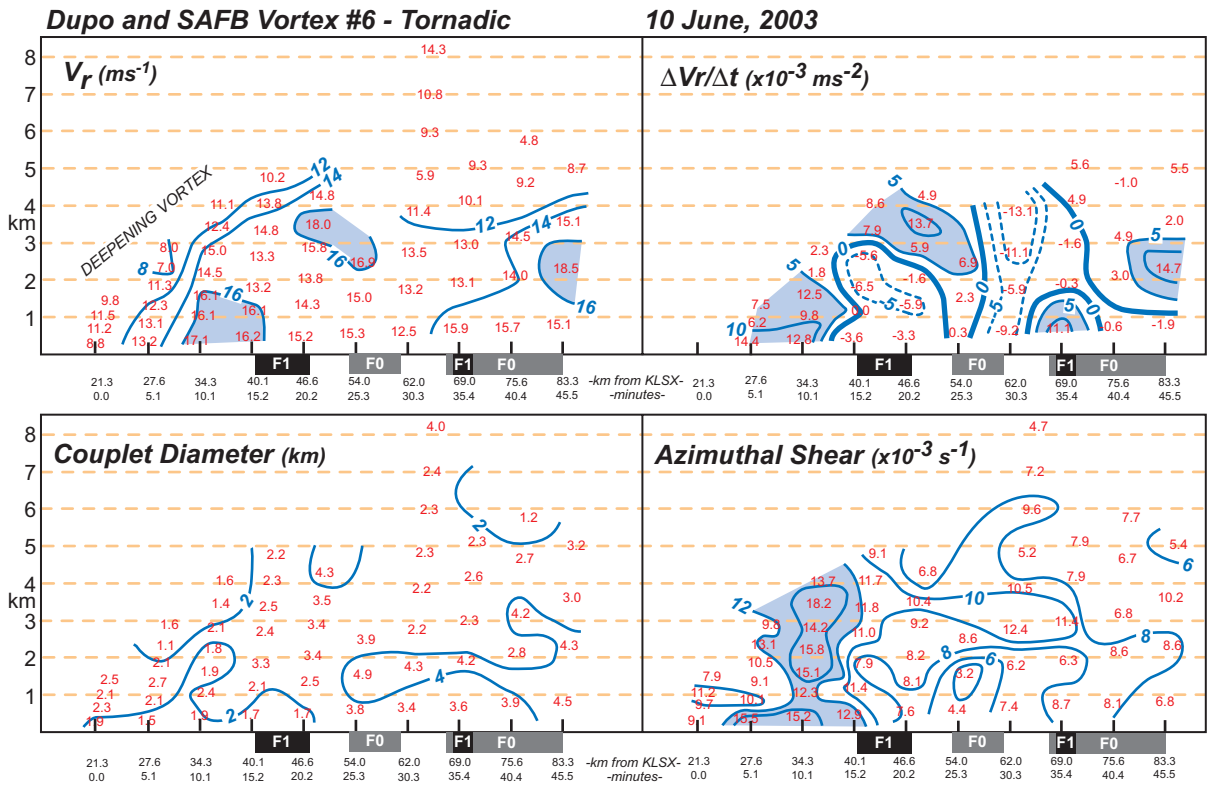

Figure 5. Time-height diagram of (a) Vr and (b) ΔVr/Δt for tornadic vortex #6 in Fig.1. Black and gray bars indicate time of tornado and straight-line wind damage, respectively.

vey analysis was carefully superimposed on the KLSX reflectivity and radial velocity data. Results of this analysis at 2300, 2310 and 2320 UTC are shown in Fig. 3. Surface wind damage was being created by 2300 UTC on the western edge of the primary damage swath. Notice that the damage swath does not appear to be collocated with the location where the core of the rear-inflow jet (RIJ), observed as a core of strong radial velocities at 2.4 degrees, is impinging upon the leading edge of the convective system. Rather, the damage is north of the RIJ core, collocated with mesovortex #6. Ten minutes later at 2310 UTC, the convective system was bowing outward between azimuths of 95° and 125° in response to the developing RIJ. The apex of the developing bow echo is defined herein as the location where the RIJ impinges on the leading edge of the convective system. At 2310 UTC, note that the primary damage swath is again *well north* of the bow apex. In fact, the radial velocity data shows that the primary damage swath is generally located on the southern periphery of mesovortex #6. This is even more evident at 2320 UTC where vortices 6 and 9 have moved closer to each other. Their combined outbound radial velocity maximum in excess of 40 ms^{-1}, is coincident with the primary damage swath location. Interestingly, vortex #6 passed directly over the BAMEX Operations Center at the Mid America Airport and adjoining Scott Airforce Base where wind gusts in excess of 45 ms^{-1} were measured. By 2325 UTC, mesovortex #6 merges with vortex #9 and dissipates after 2330 UTC (not shown). After 2330 UTC, the damage swath was likely created by the dissipating merged vortex acting constructively with embedded microbursts evident by the divergent southwesterly flow within the latter part of the primary damage swath. The results in Fig. 3 conclusively show that *low-level mesovortices within bow echoes are capable of producing long swaths of damaging straight-line winds north of the bow echo apex*. In fact, very little damage was observed along the apex of bow echo #2.

4. TORNADIC AND NONTORNADIC MESOVORTEX STRUCTURE

Apparent in Fig. 1 is that all of the tornadoes produced by the MCS were associated with the mesovortices, however, only five of the eleven circulations were tornadic. An important detection and warning question concerns whether there are any structural differences that discern the tornadic mesovortices from their nontornadic counterparts. Indeed, Atkins et al. (2004) found that tornadic mesovortices within bow echoes tend to be longer lived,

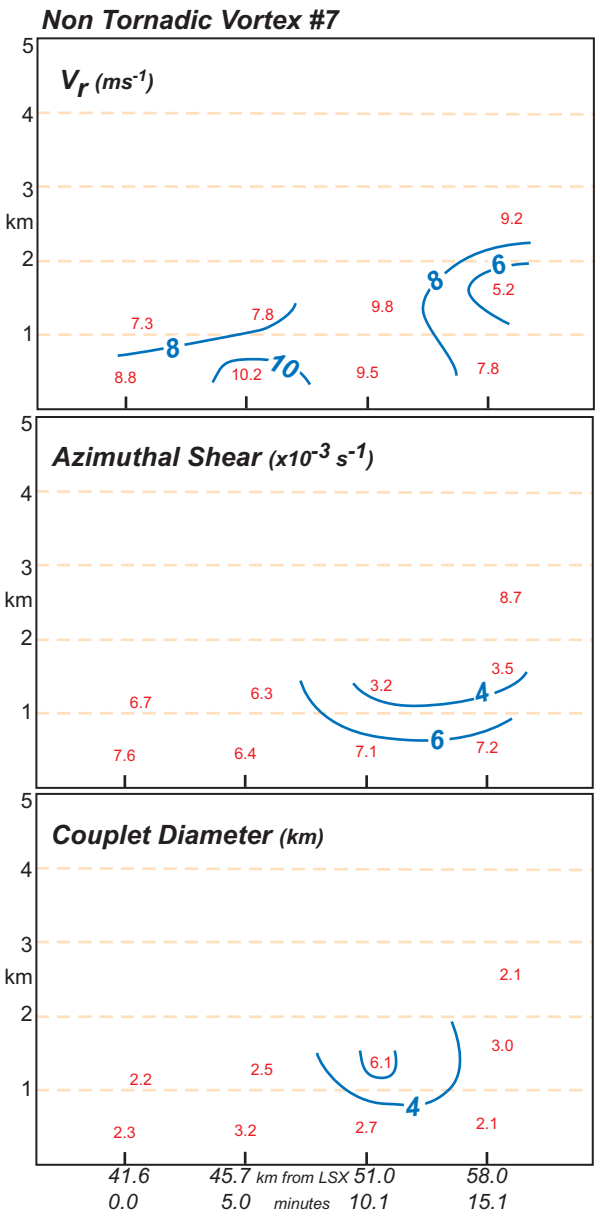

Figure 6. Time-height diagram of Vr for nontornadic vortex #7.

stronger at lower levels (0-3 km AGL), and deeper than nontornadic mesovortices. Analysis of the mesovortices shown in Fig. 1 confirms the findings of Atkins et al. (2004). The histogram of vortex lifetimes in Fig. 4c reveals that that tornadic vortices are longer lived. The mean lifetime of the tornadic (nontornadic) mesovortices was 56 (19) minutes. When comparing vortex strength (herein defined as the magnitude of V_r, see Fig. 4 caption for definition), the tornadic vortices were stronger at lower levels as shown in Fig. 4a. Plotted are the mean vortex strengths versus height for all tornadic and nontornadic mesovortices. Only data prior to tornadogenesis was used for the tornadic vortices. Fig. 4a clearly shows that vortex strength is larger from 0-3 km AGL for the tornadic vortices. The same result is found if data throughout the entire tornadic vortex lifetime is used to create the V_r profile (Fig. 4b).

Another key difference between the vortices is how they evolve with time. The tornadic vortex structure consistently evolved in a manner similar to that shown in Fig. 5. Prior to tornadogenesis, the tornadic vortices were observed to strengthen rapidly at low levels and deepen. The low-level intensification of the vortex is clearly evident in the $\Delta Vr/\Delta t$ and azimuthal shear fields shown in Fig. 5. Notice the positive values of $\Delta Vr/\Delta t$ at levels below 3 km AGL prior to the first F1 tornado. Another local maximum can be found at low levels just prior to the second tornado. This deepening and rapid vortex intensification at low levels was not observed with any of the nontornadic mesovortices. Interestingly, couplet diameter slowly increased with time. Fig. 6 shows the evolution of V_r, azimuthal shear, and couplet diameter for nontornadic vortex #7. Clearly, the V_r values are weaker, show no signs of intensification with time, and suggest a shallow vortex relative to the tornadic vortices. The evolution of vortex #7 is representative of the other nontornadic mesovortices.

5. CONCLUSIONS

Detailed damage survey and Doppler radar data were analyzed to better understand the mechanism(s) that created a 50 km long damage swath within the 10 June 2003 Saint Louis bow echo observed during BAMEX. Results of the analysis clearly showed that the damage swath was not located at the apex of the bow, rather it was displaced well north of the apex and was collocated with a mesovortex. This finding is illustrated in the schematic diagram shown in Fig. 7.

Analysis of the Doppler radar data also confirms the findings of Atkins et al. (2004) in that *it appears to be possible to distinguish between the tornadic and non tornadic mesovortices*. Consistently, the tornadic vortices were longer lived, stronger at low levels (0-3 km) and deepened rapidly just prior to tornadogenesis. The nontornadic vortices did not evolve in a similar manner.

The results of this study suggest that monitoring mesovortices within bow echoes may be an important task in the detection and warning process. Swaths of “straight-line” wind damage may be found north of the bow apex associated with a mesovortex. Furthermore, by monitoring the structural evolution of the vortices, it

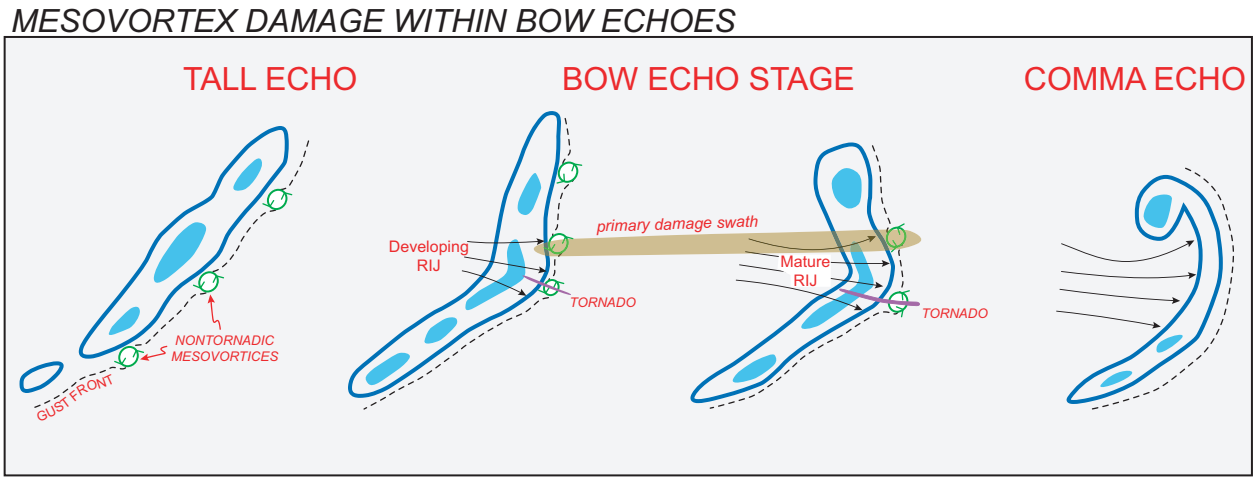

Figure 7. Schematic model of damage produced by the 10 June Saint Louis bow echo.

may be possible to determine which ones will become tornadic. This knowledge would likely lead to improved warnings of damaging winds and tornadoes.

Acknowledgements: The research results presented herein were supported by the National Science Foundation under Grant ATM-0233178 (NTA) and ATM-0233344 (RJT).

References

Atkins, N.T., and R.W. Przybylinski, 2002: Radar and damage analysis of the 27 May 2000 tornadic derecho event. Preprints, *21st Conf. on Severe Local Storms,* San Antonio, TX, Amer. Meteor. Soc., 567-570.

Atkins, N.T., J.M. Arnott, R.W. Przybylinski, R.A. Wolf, and B.D. Ketcham, 2004: Vortex structure and evolution within bow echoes. Part I: Single-Doppler and damage analysis of the 29 June 1998 Derecho. *Mon. Wea. Rev.*, **132**, 2224-2242.

Davis, C. and co-authors, 2004: The Bow Echo and MCV Experiment (BAMEX): Observations and opportunities. *Bull. Amer. Metero. Soc.,* in press.

Fujita, T.T., 1978: Manual of downburst identification for project Nimrod. Satellite and Mesometeorology Research Paper 156, Dept. of Geophysical Sciences, University of Chicago, 104 pp. [NTIS PB-286048]

Przybylinski, R.W., G.K. Schmocker, and Y-J. Lin, 2000: A study of storm and vortex morphology during the 'intensifying stage' of severe wind mesoscale convective systems. Preprints, *20th Conf. on Severe Local Storms,* Orlando, FL, Amer. Meteor. Soc., 173-176.

Schmocker, G.K., R.W. Przybylinski, and E.N. Rasmussen, 2000: The severe bow echo event of 14 June 1998 over the mid-Mississippi valley region: A case of vortex development near the intersection of a preexisting boundary and a convective line. Preprints, *20th Conf. on Severe Local Storms,* Orlando, FL, Amer. Meteor. Soc., 169-172.

Trapp, R.J. and M.L. Weisman, 2003: Low-level mesovortices within squall lines and bow echoes. Part II: Their genesis and implications. *Mon. Wea. Rev.*, **131**, 2804-2823.